49th IEEE Conference on Decision and Control
December 15-17, 2010
Hilton Atlanta Hotel, Atlanta, GA, USA

Retrospective Cost Adaptive Control of a Planar Multilink Arm with Nonminimum-Phase Zeros

Alexey V. Morozov[1], Jesse B. Hoagg[2], and Dennis S. Bernstein[3]

***Abstract*— We address the problem of adaptive command following and disturbance rejection for a nonlinear planar multilink mechanism interconnected by torsional springs and dashpots. We consider a nonlinear multilink mechanism where a control torque is applied to the hub of the multilink mechanism, and the objective is to control the angular position of the tip, which is separated from the hub by N links. In this paper, we derive the nonlinear equations of motion for the N link mechanism. We linearize these equations of motion and demonstrate that such systems have nonminimum-phase zeros when the control torque and angular position sensor are not colocated. To control this mechanism, we use a retrospective cost adaptive controller, which is effective for nonminimum-phase systems provided that you have an estimate of the nonminimum-phase zeros. We consider both command following and disturbance rejection problems, where the spectrum of the commands and disturbance are unknown.**

I. Introduction

Nonminimum-phase zeros present a fundamental impediment to the achievable performance of a closed-loop system, limiting the bandwidth and, in the case of positive zeros, causing initial undershoot or direction reversals under step inputs [1, p. 289], [2], [3]. Nonminimum-phase zeros are also challenging for adaptive control methods, which typically assume that the plant is minimum phase [4]. For discrete-time systems with nonminimum-phase zeros, the adaptive control method in [5], [6] requires that the nonminimum-phase zeros be known.

In view of these challenges, it is of interest to determine physical properties that give rise to nonminimum-phase zeros. It is known that the transfer function of a flexible structure with colocated force actuation and velocity sensing is positive real and thus minimum phase [7]. This property suggests that noncolocation is the underlying cause of nonminimum-phase zeros. It was shown in [8], however, that, for a string of translating masses interconnected by springs and dashpots, the noncolocated transfer functions between every pair of masses are minimum phase. Therefore, noncolocation per se is not the source of nonminimum phase zeros.

A vehicle with rear-wheel steering, or, equivalently, a car driving in reverse, exhibits initial undershoot in the sense that the driver initially moves in the direction that is opposite to the ultimate direction of motion. This example, as well as the examples in [9], [10], suggest that nonminimum phase zeros may arise from a combination of noncolocation and rotational motion.

In place of the translating masses considered in [8], we thus consider a planar multilink mechanism with rotating masses interconnected by torsional stiffnesses and dashpots. This mechanism can be viewed as a lumped approximation of a flexible rotating arm, whose dynamics and control are widely studied for applications such as space structures and hard drives [11], [12].

The multilink mechanism is nonlinear, and thus the derivation of its equations of motion is more complicated than the case of translating masses considered in [8], whose dynamics are linear. Analysis of the zeros of the rotating masses must therefore be based on a linearized model. A related analysis is given in [9].

For the linearized model of the rotating masses we show that the damping and stiffness matrices have the same form as in the case of translating masses. However, the key difference between the translational and rotational cases is the inertia matrix, which is diagonal for the translating masses but nondiagonal for the rotating masses. With this distinction in mind, the first objective of this paper is to revisit the analysis of [8] and show how the off-diagonal entries of the inertia matrix for the rotating masses give rise to nonminimum-phase zeros.

Next, we consider adaptive control of the planar multilink mechanism using the approach of [6]. Since this method requires knowledge of the nonminimum-phase zeros, we assume that this information is available, either by analytical modeling or system identification [13]. We then apply the retrospective adaptive control algorithm of [6] on both the linearized and nonlinear system and assess the resulting performance for problems of command following and disturbance rejection.

II. Nonlinear Equations of Motion

In this section, we derive the nonlinear equations of motion for an N-link planar arm system by using Lagrange's equations. First, we define the parameters of the system. Let p_1 be the point where the first link is connected to the horizontal plane, and, for $n = 2, ..., N$, let p_n be the point where the $n^{\rm th}$ link is connected to the $(n-1)^{\rm th}$ link. Next, for $n = 1, ..., N$, let q_n be the center of mass of the $n^{\rm th}$ link. Furthermore, for $n = 1, ..., N$, let m_n be the mass of the $n^{\rm th}$ link, let l_n be the length of the $n^{\rm th}$ link, let c_n be the damping at the joint p_n, let k_n be the stiffness of the

[1]Graduate Student, Department of Aerospace Engineering, University of Michigan, email: morozova@umich.edu

[2]Assistant Professor, Department of Mechanical Engineering, University of Kentucky, email: jhoagg@engr.uky.edu

[3]Professor, Department of Aerospace Engineering, University of Michigan, email: dsbaero@umich.edu

978-1-4244-7744-9/10/$26.00 ©2010 IEEE

joint p_n, and let $I_n \triangleq \frac{1}{12}m_n l_n^2$ be the moment of inertia of the n^{th} link about q_n.

Next, we define the inertial frame F_A with orthogonal unit vectors $(\hat{\imath}_{\mathrm{A}}, \hat{\jmath}_{\mathrm{A}}, \hat{k}_{\mathrm{A}})$, where $\hat{\imath}_{\mathrm{A}}$ and $\hat{\jmath}_{\mathrm{A}}$ lie in the plane of motion of the N-link planar arm, and $\hat{k}_{\mathrm{A}}$ is orthogonal to the plane of motion. For simplicity, we assume that the origin of $\mathrm{F_A}$ is located at p_1. In addition, for $n = 1, ..., N$, let $\mathrm{F}_{\mathrm{B}_n}$ be a frame attached to the n^{th} link. More specifically, $\mathrm{F}_{\mathrm{B}_n}$ is a body-fixed frame which rotates as the n^{th} link rotates. For $n = 1, \ldots, N$, let $\mathrm{F}_{\mathrm{B}_n}$ have orthogonal unit vectors $(\hat{\imath}_{\mathrm{B}_n}, \hat{\jmath}_{\mathrm{B}_n}, \hat{k}_{\mathrm{B}_n})$, where $\hat{\imath}_{\mathrm{B}_n}$ is in the direction from p_1 to q_1, $\hat{\jmath}_{\mathrm{B}_n}$ is orthogonal to $\hat{\imath}_{\mathrm{B}_n}$ and in the plane of motion, and $\hat{k}_{\mathrm{B}_n}$ is orthogonal to the plane of motion. Note that, for all $n = 1, \ldots, N$, $\hat{k}_{\mathrm{B}_n} = \hat{k}_{\mathrm{A}}$. Finally, for $n = 1, \ldots, N$, let θ_n be the angle from $\hat{\imath}_{\mathrm{A}}$ to $\hat{\imath}_{\mathrm{B}_n}$. The N-link planar arm is shown in Figure 1. To construct the Lagrangian for the N-link system, we derive expressions for kinetic and potential energies, and thus we require the translational and rotational velocities of each linkage. For $n = 1, \ldots, N$, the rotational velocity of $\mathrm{F}_{\mathrm{B}_n}$ with respect to $\mathrm{F_A}$ resolved in $\mathrm{F_A}$ is given by $\omega_n \triangleq \vec{\omega}_{\mathrm{B}_n/\mathrm{A}}\big|_{\mathrm{A}} = \begin{bmatrix} 0 & 0 & \dot{\theta}_n \end{bmatrix}^{\mathrm{T}}$. Furthermore, for $n = 1, \ldots, N$, the orientation matrix of $\mathrm{F}_{\mathrm{B}_n}$ with respect to $\mathrm{F_A}$ is given by

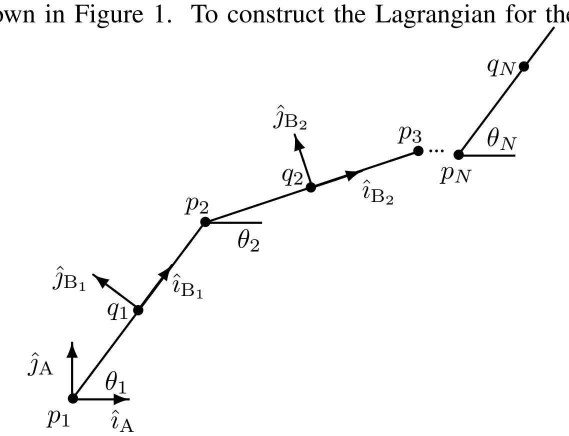

Fig. 1. N-link planar arm system. All motion is in the horizontal plane.

$$\mathcal{O}_{\mathrm{B}_n/\mathrm{A}} = \begin{bmatrix} \cos(\theta_n) & \sin(\theta_n) & 0 \\ -\sin(\theta_n) & \cos(\theta_n) & 0 \\ 0 & 0 & 1 \end{bmatrix}. \tag{1}$$

Next, for $n = 1, \ldots, N$, let $\vec{r}_{q_n/p_1}$ be the position vector from p_1 to q_n. For $n = 1, \ldots, N$, the velocity of q_n relative to p_1 with respect to $\mathrm{F_A}$ is given by

$$\vec{V}_{q_n/p_1/\mathrm{A}} \triangleq \overset{\mathrm{A}\bullet}{\vec{r}}_{q_n/p_1} = \overset{\mathrm{A}\bullet}{\vec{r}}_{q_n/p_n} + \sum_{i=1}^{n-1} \overset{\mathrm{A}\bullet}{\vec{r}}_{p_{i+1}/p_i}, \tag{2}$$

where $\overset{\mathrm{A}\bullet}{\vec{r}}$ denotes the derivative of $\vec{r}$ taken in the frame $\mathrm{F_A}$. Next, we apply the transport theorem to each term in (2), which yields

$$\vec{V}_{q_n/p_1/\mathrm{A}} = \left(\overset{\mathrm{B}_n\bullet}{\vec{r}}_{q_n/p_n} + \vec{\omega}_{\mathrm{B}_n/\mathrm{A}} \times \vec{r}_{q_n/p_n} \right) + \sum_{i=1}^{n-1} \left(\overset{\mathrm{B}_i\bullet}{\vec{r}}_{p_{i+1}/p_i} + \vec{\omega}_{\mathrm{B}_i/\mathrm{A}} \times \vec{r}_{p_{i+1}/p_i} \right).$$

Note that, for $n = 1, \ldots, N$, $\vec{r}_{q_n/p_n}$ is fixed relative to $\mathrm{F}_{\mathrm{B}_n}$, and thus $\overset{\mathrm{B}_n\bullet}{\vec{r}}_{q_n/p_n} = 0$. Furthermore, note that for $i = 1, \ldots, N-1$ $\vec{r}_{p_{i+1}/p_i}$ is fixed relative to B_i, and thus $\overset{\mathrm{B}_i\bullet}{\vec{r}}_{p_{i+1}/p_i} = 0$. Therefore,

$$\vec{V}_{q_n/p_1/\mathrm{A}} = \vec{\omega}_{\mathrm{B}_n/\mathrm{A}} \times \vec{r}_{q_n/p_n} + \sum_{i=1}^{n-1} \vec{\omega}_{\mathrm{B}_i/\mathrm{A}} \times \vec{r}_{p_{i+1}/p_i}.$$

For $n = 1, \ldots, N$, resolving $\vec{V}_{q_n/p_1/\mathrm{A}}$ in $\mathrm{F_A}$ yields

$$\begin{aligned} \vec{V}_{q_n/p_1/\mathrm{A}}\Big|_{\mathrm{A}} &= \vec{\omega}_{\mathrm{B}_n/\mathrm{A}}\Big|_{\mathrm{A}}^{\times} \vec{r}_{q_n/p_n}\Big|_{\mathrm{A}} \\ &\quad + \sum_{i=1}^{n-1} \vec{\omega}_{\mathrm{B}_i/\mathrm{A}}\Big|_{\mathrm{A}}^{\times} \vec{r}_{p_{i+1}/p_i}\Big|_{\mathrm{A}}, \end{aligned} \tag{3}$$

where, for $n = 1, \ldots, N$,

$$\vec{\omega}_{\mathrm{B}_n/\mathrm{A}}\Big|_{\mathrm{A}}^{\times} = \begin{bmatrix} 0 & -\dot{\theta}_n & 0 \\ \dot{\theta}_n & 0 & 0 \\ 0 & 0 & 0 \end{bmatrix}, \tag{4}$$

$$\vec{r}_{q_n/p_n}\Big|_{\mathrm{A}} = \mathcal{O}_{\mathrm{B}_n/\mathrm{A}} \begin{bmatrix} \frac{l_n}{2} & 0 & 0 \end{bmatrix}^{\mathrm{T}}, \tag{5}$$

and, for $n = 1, \ldots, N-1$,

$$\vec{r}_{p_{n+1}/p_n}\Big|_{\mathrm{A}} = \mathcal{O}_{\mathrm{B}_n/\mathrm{A}} \begin{bmatrix} l_n & 0 & 0 \end{bmatrix}^{\mathrm{T}}. \tag{6}$$

Furthermore, for $n = 1, \ldots, N$, define $V_n \triangleq \left\| \vec{V}_{q_n/p_1/\mathrm{A}}\Big|_{\mathrm{A}} \right\|$. For demonstration, it follows from (3)-(6) that

$$\begin{aligned} \vec{V}_{q_1/p_1/\mathrm{A}}\Big|_{\mathrm{A}} &= \begin{bmatrix} 0 & -\dot{\theta}_1 & 0 \\ \dot{\theta}_1 & 0 & 0 \\ 0 & 0 & 0 \end{bmatrix} \mathcal{O}_{\mathrm{B}_1/\mathrm{A}} \begin{bmatrix} \frac{l_1}{2} \\ 0 \\ 0 \end{bmatrix} \\ &= \begin{bmatrix} -\frac{1}{2} l_1 \sin(\theta_1)\dot{\theta}_1 \\ \frac{1}{2} l_1 \cos(\theta_1)\dot{\theta}_1 \\ 0 \end{bmatrix}, \end{aligned}$$

and thus $V_1 = \frac{1}{2} l_1 \dot{\theta}_1$. Following this same procedure for $n \geq 2$, yields, for $n = 1, \ldots, N$,

$$V_n = \left[\tfrac{1}{4} l_n^2 \dot{\theta}_n^2 + \sum_{i=1}^{n-1} \left(l_i^2 \dot{\theta}_i^2 + l_n l_i \dot{\theta}_n \dot{\theta}_i \cos(\theta_i - \theta_n) \right) + 2 \sum_{i \neq j}^{n-1} l_i l_j \dot{\theta}_i \dot{\theta}_j \cos(\theta_i - \theta_j) \right]^{1/2}. \tag{7}$$

For $n = 1, \ldots, N$, the kinetic energy of the n^{th} link is

$$\begin{aligned} T_n &\triangleq \tfrac{1}{2} m_n V_n^2 + \tfrac{1}{2} I_n \|\omega_n\|^2 \\ &= \tfrac{m_n}{2} \left(\tfrac{1}{3} l_n^2 \dot{\theta}_n^2 + \sum_{i=1}^{n-1} \left(l_i^2 \dot{\theta}_i^2 + l_n l_i \dot{\theta}_n \dot{\theta}_i \cos(\theta_i - \theta_n) \right) \right. \\ &\quad \left. + 2 \sum_{i \neq j}^{n-1} l_i l_j \dot{\theta}_i \dot{\theta}_j \cos(\theta_i - \theta_j) \right), \end{aligned} \tag{8}$$

and the total kinetic energy is defined by $T \triangleq \sum_{n=1}^{N} T_n$. Next, for $n = 1, \ldots, N$, the potential energy of the n^{th} link is

$$U_n \triangleq \begin{cases} \frac{1}{2}k_1\theta_1^2, & n=1, \\ \frac{1}{2}k_n(\theta_{n-1}-\theta_n)^2, & n>1, \end{cases} \tag{9}$$

and the total potential energy is defined by $U \triangleq \sum_{n=1}^{N} U_n$.

Thus, the Lagrangian for the N-link system is $L \triangleq T - U$. Next, for $n = 1, \ldots, N$, let F_{c_n} be the dissipative torque resulting from the damping at joint p_n, that is,

$$F_{c_n} \triangleq \begin{cases} \frac{1}{2}c_1\dot{\theta}_1^2, & n=1, \\ \frac{1}{2}c_n(\dot{\theta}_{n-1}-\dot{\theta}_n)^2, & n>1. \end{cases} \tag{10}$$

Furthermore, for $n = 1, \ldots, N$, let u_n be an external torque applied at p_n. Therefore, for $n = 1, \ldots, N$ the nonlinear equations of motion are given by

$$\frac{d}{dt}\frac{\partial L}{\partial \dot{\theta}_n} - \frac{\partial L}{\partial \theta_n} + \frac{\partial F_{c_n}}{\partial \dot{\theta}_n} = u_n. \tag{11}$$

Now, we specialize to the case where $N = 2$. In this case, the Lagrangian is

$$\begin{aligned} L = {} & \tfrac{1}{2}m_1(\tfrac{1}{3}l_1^2\dot{\theta}_1^2) - \tfrac{1}{2}k_1\theta_1^2 - \tfrac{1}{2}k_2(\theta_1-\theta_2)^2 \\ & + \tfrac{1}{2}m_2(\tfrac{1}{3}l_2^2\dot{\theta}_2^2 + l_1^2\dot{\theta}_1^2 + l_1l_2\dot{\theta}_1\dot{\theta}_2\cos(\theta_1-\theta_2)), \end{aligned} \tag{12}$$

and it follows from (11) and (12) that the equations of motion are given by

$$\begin{aligned} u_1 = {} & (\tfrac{1}{3}m_1l_1^2 + m_2l_1^2)\ddot{\theta}_1 + \tfrac{1}{2}m_2l_1l_2\sin(\theta_1-\theta_2)\dot{\theta}_2^2 \\ & + \tfrac{1}{2}m_2l_1l_2\cos(\theta_1-\theta_2)\ddot{\theta}_2 + (k_1+k_2)\theta_1 - k_2\theta_2 \\ & + (c_1+c_2)\dot{\theta}_1 - c_2\dot{\theta}_2, \end{aligned} \tag{13}$$

$$\begin{aligned} u_2 = {} & (\tfrac{1}{3}m_2l_2^2)\ddot{\theta}_2 - \tfrac{1}{2}m_2l_1l_2\sin(\theta_1-\theta_2)\dot{\theta}_1^2 \\ & + \tfrac{1}{2}m_2l_1l_2\cos(\theta_1-\theta_2)\ddot{\theta}_1 - k_2\theta_1 + k_2\theta_2 \\ & - c_2\dot{\theta}_1 + c_2\dot{\theta}_2. \end{aligned} \tag{14}$$

III. Linearized Equations of Motion

In this section, we derive linearized equations of motion for N-link system. First, we linearize the equations of motion for the two-link case. Then, we linearize the equations of motion for the three-link case. Finally, we generalize the linear equations of motion to the N-link case.

First, define

$$\Theta \triangleq \begin{bmatrix} \theta_1 & \ldots & \theta_N \end{bmatrix}^{\mathrm{T}}, \ \Upsilon \triangleq \begin{bmatrix} u_1 & \ldots & u_N \end{bmatrix}^{\mathrm{T}}.$$

We linearize about the $(\Theta, \dot{\Theta}) \equiv 0$ equilibrium. Note that if, for all $n = 1, ..., N$, $k_n > 0$, then $(\Theta, \dot{\Theta}) \equiv 0$ is the only equilibrium of the N-link system . Let $\delta\Theta$ be the linear approximation of Θ around the equilibrium $(\Theta, \dot{\Theta}) \equiv 0$. To obtain the linearization, we use the small angle approximations $\sin(\theta_1 - \theta_2) \approx \delta\theta_1 - \delta\theta_2$, $\cos(\theta_1 - \theta_2) \approx 1$.

Linearizing the two-link system, with nonlinear equations of motion (13) and (14), about $(\Theta, \dot{\Theta}) \equiv 0$ yields

$$M\delta\ddot{\Theta} + C_d\delta\dot{\Theta} + K\delta\Theta = \Upsilon, \tag{15}$$

where

$$M \triangleq \begin{bmatrix} (\frac{m_1}{3}+m_2)l_1^2 & \frac{m_2}{2}l_2l_1 \\ \frac{m_2}{2}l_1l_2 & \frac{m_2}{3}l_2^2 \end{bmatrix},$$

$$C_d \triangleq \begin{bmatrix} c_1+c_2 & -c_2 \\ -c_2 & c_2 \end{bmatrix}, K \triangleq \begin{bmatrix} k_1+k_2 & -k_2 \\ -k_2 & k_2 \end{bmatrix}.$$

Similarly, linearizing the three-link system about $(\Theta, \dot{\Theta}) \equiv 0$ yields (15), where

$$M \triangleq \begin{bmatrix} (\frac{m_1}{3}+m_2+m_3)l_1^2 & (\frac{m_2}{2}+m_3)l_2l_1 & \frac{m_3}{2}l_1l_3 \\ (\frac{m_2}{2}+m_3)l_1l_2 & (\frac{m_2}{3}+m_3)l_2^2 & \frac{m_3}{2}l_2l_3 \\ \frac{m_3}{2}l_1l_3 & \frac{m_3}{2}l_2l_3 & \frac{m_3}{3}l_3^2 \end{bmatrix},$$

$$C_d \triangleq \begin{bmatrix} c_1+c_2 & -c_2 & 0 \\ -c_2 & c_2+c_3 & -c_3 \\ 0 & -c_3 & c_3 \end{bmatrix},$$

$$K \triangleq \begin{bmatrix} k_1+k_2 & -k_2 & 0 \\ -k_2 & k_2+k_3 & -k_3 \\ 0 & -k_3 & k_3 \end{bmatrix}.$$

Finally, extending this technique, we obtain the linearization for the N-link system, which is given by (15), where

$$M \triangleq \begin{bmatrix} \gamma_{1,1} & \cdots & \gamma_{1,N} \\ \vdots & \ddots & \vdots \\ \gamma_{N,1} & \cdots & \gamma_{N,N} \end{bmatrix},$$

$$C_d \triangleq \begin{bmatrix} c_1+c_2 & -c_2 & 0 & \ldots & 0 \\ -c_2 & c_2+c_3 & -c_3 & \ldots & 0 \\ 0 & -c_3 & c_3+c_4 & \ldots & 0 \\ \vdots & \vdots & \vdots & \ddots & \vdots \\ 0 & 0 & 0 & \ldots & c_N \end{bmatrix},$$

$$K \triangleq \begin{bmatrix} k_1+k_2 & -k_2 & 0 & \ldots & 0 \\ -k_2 & k_2+c_3 & -k_3 & \ldots & 0 \\ 0 & -k_3 & k_3+k_4 & \ldots & 0 \\ \vdots & \vdots & \vdots & \ddots & \vdots \\ 0 & 0 & 0 & \ldots & k_N \end{bmatrix},$$

where, for $g = 1, ..., N$,

$$\gamma_{g,g} \triangleq \left(\frac{m_g}{3} + \sum_{i=g+1}^{N} m_i\right) l_g^2, \tag{16}$$

and, for $g = 1, ..., N$ and $h = g+1, ..., N$,

$$\gamma_{g,h} \triangleq \left(\frac{m_h}{2} + \sum_{i=h+1}^{N} m_i\right) l_g l_h, \tag{17}$$

and, for $g, h = 1, ..., N$, $\gamma_{h,g} = \gamma_{g,h}$.

IV. Nonminimum-Phase Zeros of the N-Link Arm

In this section, we prove that, for the two-link system, the linear transfer function from u_1 to $\delta\theta_2$ has one nonminimum phase zero. In fact, this transfer function has one positive zero. For the N-link system, we numerically demonstrate that the linear transfer function from u_1 to $\delta\theta_N$ (i.e., from the hub to the tip of the multilink mechanism) has $N-1$ nonminimum-phase zeros.

For the N-link system, the linearized equations of motion (15) can be written as

$$\begin{bmatrix} \delta\dot{\Theta} \\ \delta\ddot{\Theta} \end{bmatrix} = A \begin{bmatrix} \delta\Theta \\ \delta\dot{\Theta} \end{bmatrix} + B\Upsilon, \tag{18}$$

where

$$A \triangleq \begin{bmatrix} 0_{N\times N} & I_N \\ -M^{-1}K & -M^{-1}C_d \end{bmatrix}, B \triangleq \begin{bmatrix} 0_{N\times N} \\ M^{-1} \end{bmatrix}.$$

Next, for $n = 2, \ldots, N$, the transfer function from u_1 to $\delta\theta_n$ is given by

$$G_n(s) \triangleq \frac{\delta\theta_n(s)}{u_1(s)} = C_n(sI_N - A)^{-1}B_1, \qquad (19)$$

where

$$C_n \triangleq \begin{bmatrix} 0_{1\times n-1} & 1 & 0_{1\times 2N-n} \end{bmatrix}, \quad B_1 \triangleq B \begin{bmatrix} 1 \\ 0_{1\times N-1} \end{bmatrix}.$$

For the two-link case (i.e., $N = 2$), the transfer function from u_1 to $\delta\theta_2$ can be expressed as

$$G_2(s) = \frac{\delta\theta_2(s)}{u_1(s)} = \frac{a_2 s^2 + a_1 s + a_0}{b_4 s^4 + b_3 s^3 + b_2 s^2 + b_1 s + b_0},$$

where the coefficients $a_0, \ldots, a_2, b_0, \ldots, b_4$ depend on the physical parameters of the system. More specifically, the numerator coefficients of $G_2(s)$ are given by $a_2 = -18 l_1 l_2 m_2, a_1 = 36 c_2, a_0 = 36 k_2$. Since the zeros of $G_2(s)$ are the roots of the quadratic polynomial $a_2 s^2 + a_1 s + a_0$, we can solve for these roots expressed in the physical parameters of the system. More specifically, the quadratic polynomial $a_2 s^2 + a_1 s + a_0$ has the roots $z_{c,1} = \frac{c_2 + \sqrt{c_2^2 + 2k_2 l_1 l_2 m_2}}{l_1 l_2 m_2}$ and $z_{c,2} = \frac{c_2 - \sqrt{c_2^2 + 2k_2 l_1 l_2 m_2}}{l_1 l_2 m_2}$. Since the physical parameters l_1, l_2, m_2, c_2, and k_2 are positive, it follows that $z_{c,1}$ is positive and $z_{c,2}$ is negative. Thus, we conclude that $G_2(s)$ has one nonminimum-phase zero.

For the N-link case, where $N > 2$, we conduct a numerical study to investigate the properties of the zeros of the transfer function from u_1 to $\delta\theta_N$. In particular, we let $N = 3, \ldots, 10$, and for each value of N, we randomly generate 10,000 multilink systems. For each of the multilink systems, the masses $m_1, \ldots, m_N$, the stiffnesses $k_1, \ldots, k_N$, the damping coefficients $c_1, \ldots, c_N$, and the lengths $l_1, \ldots, l_N$ are sampled from a uniformly generated random variable on the interval $(0, 100]$. Next, we compute the linearized transfer function $G_N(s)$ from u_1 to $\delta\theta_N$. For $N = 3, \ldots, 10$, all 10,000 randomly generated multilink systems have $N - 1$ nonminimum-phase zeros in the transfer function $G_N(s)$. In fact, all of the randomly generated multilink systems have $N - 1$ positive zeros in the transfer function $G_N(s)$. Future work will include a proof of the conjecture that, for an N-link system, the linearized transfer function $G_N(s)$ from the control torque at the hub to the angular position of the N^{th} link has $N - 1$ positive zeros.

Next, we discretize $G_2(s)$ using a zero-order hold on the inputs. For this example, we consider the system parameters given by $m_1 = 2$ kg, $m_2 = 1$ kg, $l_1 = 3$ m, $l_2 = 2$ m, $k_1 = 7\ \frac{\text{N}-\text{m}}{\text{rad}}$, $k_2 = 5\ \frac{\text{N}-\text{m}}{\text{rad}}$, $c_1 = 10\ \frac{\text{kg}-\text{m}^2}{\text{rad}}$, and $c_2 = 1\ \frac{\text{kg}-\text{m}^2}{\text{rad}}$.

Discretizing $G_2(s)$ using a zero-order hold on the inputs results in a discrete-time transfer function, which also has one nonminimum-phase zero. The location of this nonminimum-phase zero depends on the sampling time used for the discretization. The discrete-time nonminimum-phase zero of $G_2(z)$ with the system parameters above and sampled at a rate of 20Hz is located at approximately 1.08. Furthermore, note that the discrete-time system has one zero, which results from sample data effects. In this case, the sampled-data zero is located at -0.94.

V. Review of the Adaptive Controller

In this section, we review the cumulative retrospective cost adaptive controller presented in [6]. First, consider the multi-input, multi-output discrete-time system

$$x(k+1) = Ax(k) + Bu(k) + D_1 w(k), \qquad (20)$$
$$y(k) = Cx(k) + Du(k) + D_2 w(k), \qquad (21)$$
$$z(k) = E_1 x(k) + E_2 u(k) + E_0 w(k), \qquad (22)$$

where $x(k) \in \mathbb{R}^n$, $y(k) \in \mathbb{R}^{l_y}$, $z(k) \in \mathbb{R}^{l_z}$, $u(k) \in \mathbb{R}^{l_u}$, $w(k) \in \mathbb{R}^{l_w}$, and $k \geq 0$. Our goal is to develop an adaptive controller that generates a control signal u that minimizes the performance z in the presence of the exogenous signal w. We assume that measurements of y and z are available for feedback; however, we assume that a direct measurement of w is not available. Note that w can represent either a command signal to be followed, an external disturbance to be rejected, or both.

We represent (20) and (22) as the time-series model from u and w to z given by

$$z(k) = \sum_{i=1}^{n} -\alpha_i z(k-i) + \sum_{i=d}^{n} \beta_i u(k-i) + \sum_{i=0}^{n} \gamma_i w(k-i),$$

where $\alpha_1, \ldots, \alpha_n \in \mathbb{R}$, $\beta_d, \ldots, \beta_n \in \mathbb{R}^{l_z \times l_u}$, $\gamma_0, \ldots, \gamma_n \in \mathbb{R}^{l_z \times l_w}$, and the relative degree d is the smallest non-negative integer i such that the ith Markov parameter, either $H_0 \triangleq E_2$ if $i = 0$ or $H_i \triangleq E_1 A^{i-1} B$ if $i > 0$, is nonzero. Note that $\beta_d = H_d$.

Now, we present an adaptive control algorithm for the general control problem represented by (20)-(22). We use a strictly proper time-series controller of order n_c, such that the control $u(k)$ is given by

$$u(k) = \sum_{i=1}^{n_c} M_i(k) u(k-i) + \sum_{i=1}^{n_c} N_i(k) y(k-i), \qquad (23)$$

where, for all $i = 1, \ldots, n_c$, $M_i : \mathbb{N} \to \mathbb{R}^{l_u \times l_u}$ and $N_i : \mathbb{N} \to \mathbb{R}^{l_u \times l_y}$ are determined by the adaptive control law presented below. The control (23) can be expressed as $u(k) = \theta_c(k)\phi(k)$, where

$$\theta_c(k) \triangleq \begin{bmatrix} N_1(k) & \cdots & N_{n_c}(k) & M_1(k) & \cdots & M_{n_c}(k) \end{bmatrix},$$
$$\phi(k) \triangleq \begin{bmatrix} y^{\mathrm{T}}(k-1) & \cdots & y^{\mathrm{T}}(k-n_c) \\ u^{\mathrm{T}}(k-1) & \cdots & u^{\mathrm{T}}(k-n_c) \end{bmatrix}^{\mathrm{T}} \in \mathbb{R}^{n_c(l_u+l_y)}.$$

Next, we define the retrospective performance

$$\hat{z}(\hat{\theta}_c, k) \triangleq z(k) + \sum_{i=d}^{\nu} \bar{\beta}_i \left[\hat{\theta}_c - \theta_c(k-i)\right] \phi(k-i), \qquad (24)$$

where $\nu \geq d$, $\hat{\theta}_c \in \mathbb{R}^{l_u \times (n_c(l_y+l_u))}$ is an optimization variable used to derive the adaptive law, and $\bar{\beta}_d, \ldots, \bar{\beta}_\nu \in \mathbb{R}^{l_z \times l_u}$. The parameters ν and $\bar{\beta}_d, \ldots, \bar{\beta}_\nu$ must capture the information included in the first nonzero Markov parameter and the nonminimum-phase zeros from u to z [6]. In this paper, we let $\bar{\beta}_d, \ldots, \bar{\beta}_\nu$ be the coefficients of the portion of the numerator polynomial matrix $\beta(\mathbf{z}) \triangleq \mathbf{z}^{n-d}\beta_d + \mathbf{z}^{n-d-1}\beta_{d+1} + \cdots + \mathbf{z}\beta_{n-1} + \beta_n$ that includes the nonminimum-phase transmission zeros. More specifically, let $\beta(\mathbf{z})$ have the polynomial matrix factorization $\beta(\mathbf{z}) = \beta_{\rm U}(\mathbf{z})\beta_{\rm S}(\mathbf{z})$, where $\beta_{\rm U}(\mathbf{z})$ is an $l_z \times l_u$ polynomial matrix of degree $n_{\rm U} \geq 0$ whose leading matrix coefficient is β_d, $\beta_{\rm S}(\mathbf{z})$ is a monic $l_u \times l_u$ polynomial matrix of degree $n - n_{\rm U} - d$, and each Smith zero of $\beta(\mathbf{z})$ counting multiplicity that lies on or outside the unit circle is a Smith zero of $\beta_{\rm U}(\mathbf{z})$. Next, we can write $\beta_{\rm U}(\mathbf{z}) = \beta_{{\rm U},0}\mathbf{z}^{n_{\rm U}} + \beta_{{\rm U},1}\mathbf{z}^{n_{\rm U}-1} + \cdots + \beta_{{\rm U},n_{\rm U}-1}\mathbf{z} + \beta_{{\rm U},n_{\rm U}}$, where $\beta_{{\rm U},0} \triangleq \beta_d$. In this case, we let $\nu = n_{\rm U} + d$ and for $i = d, \ldots, n_{\rm U} + d$, $\bar{\beta}_i = \beta_{{\rm U},i-d}$. For other choices of the parameters ν and $\bar{\beta}_d, \ldots, \bar{\beta}_\nu$, see [6].

Defining $\hat{\Theta}_{\rm c} \triangleq \operatorname{vec} \hat{\theta}_{\rm c} \in \mathbb{R}^{n_c l_u (l_y + l_u)}$ and $\Theta_{\rm c}(k) \triangleq \operatorname{vec} \theta_{\rm c}(k) \in \mathbb{R}^{n_c l_u (l_y + l_u)}$, it follows that

$$\hat{z}(\hat{\Theta}_{\rm c}, k) = z(k) - \sum_{i=d}^{\nu} \Phi_i^{\rm T}(k)\Theta_{\rm c}(k-i) + \Psi^{\rm T}(k)\hat{\Theta}_{\rm c}, \quad (25)$$

where, for $i = d, \ldots, \nu$, $\Phi_i(k) \triangleq \phi(k-i) \otimes \bar{\beta}_i^{\rm T} \in \mathbb{R}^{(n_c l_u (l_y + l_u)) \times l_z}$, where $\otimes$ represents the Kronecker product, and $\Psi(k) \triangleq \sum_{i=d}^{\nu} \Phi_i(k)$.

Now, define the *cumulative retrospective cost function*

$$\begin{aligned} J(\hat{\Theta}_{\rm c}, k) \triangleq \sum_{i=0}^{k} & \lambda^{k-i} \hat{z}^{\rm T}(\hat{\Theta}_{\rm c}, i) R \hat{z}(\hat{\Theta}_{\rm c}, i) \\ & + \lambda^k (\hat{\Theta}_{\rm c} - \Theta_{\rm c}(0))^{\rm T} Q (\hat{\Theta}_{\rm c} - \Theta_{\rm c}(0)), \quad (26) \end{aligned}$$

where $\lambda \in (0, 1]$, and $R \in \mathbb{R}^{l_z \times l_z}$ and $Q \in \mathbb{R}^{(n_c l_u (l_y + l_u)) \times (n_c l_u (l_y + l_u))}$ are positive definite.

The cumulative retrospective cost function (26) is minimized by a recursive least-squares (RLS) algorithm with a forgetting factor [14]–[16]. Therefore, $J(\hat{\Theta}_{\rm c}, k)$ is minimized by the adaptive law

$$\Theta_{\rm c}(k+1) = \Theta_{\rm c}(k) - P(k)\Psi(k)\Omega(k)^{-1} z_{\rm R}(k), \quad (27)$$

$$P(k+1) = \frac{1}{\lambda}P(k) - \frac{1}{\lambda}P(k)\Psi(k)\Omega(k)^{-1}\Psi^{\rm T}(k)P(k), \quad (28)$$

where $\Omega(k) \triangleq \lambda R^{-1} + \Psi^{\rm T}(k)P(k)\Psi(k)$, $P(0) = Q^{-1}$, $\Theta_{\rm c}(0) \in \mathbb{R}^{n_c l_u (l_y + l_u)}$, and the retrospective performance measure $z_{\rm R}(k) \triangleq \hat{z}(\Theta_{\rm c}(k), k)$. Note that the retrospective performance measure is computable from (25) using measured signals z, y, u, $\theta_{\rm c}$, and the matrix coefficients $\bar{\beta}_d, \ldots, \bar{\beta}_\nu$. The cumulative retrospective cost adaptive control law is thus given by (27), (28), and

$$u(k) = \theta_{\rm c}(k)\phi(k) = \operatorname{vec}^{-1}(\Theta_{\rm c}(k))\phi(k). \quad (29)$$

VI. Numerical Examples

In this section, we use the retrospective cost adaptive controller (27)-(29) to control the linearized and nonlinear two-link system. In particular, we consider both the command following and disturbance rejection problems for the linearized and nonlinear two-link system. We assume that u_1 is the only available control input. We consider the two-link system with parameters given in Section IV. The adaptive controller (27)-(29) is implemented in feedback at 20Hz with $\lambda = 0.99$, $R = 1$, $n_{\rm c} = 8$, $P(0) = 10^{16} I_{16}$, and $\theta_{\rm c}(0) = 0$. Additionally, for each example, the system is allowed to run open-loop for 7.5 seconds and then the adaptive controller is turned on.

First, numerical simulations are performed using the linearized and nonlinear two-link system to asses the adaptive control's performance on a command following problem. The control objective is for θ_2 to track a 0.8 Hz sinusoid with a magnitude of 0.3 rad. We assume that the relative degree d and the first nonzero Markov parameter are known, that is, we let $\nu = d + 1$ and $\bar{\beta}_d = H_d$. In this example, $d = 1$ and $H_d = -0.00032$. In addition, we assume that the location of the nonminimum-phase zero is known, but no other information about the system is assumed to be known. Figure 2 shows that the adaptive controller drives performance variable z to zero.

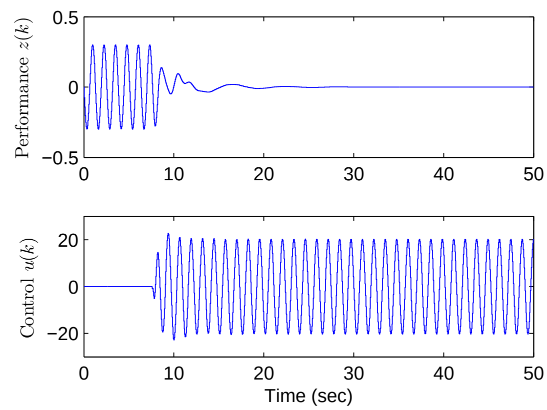

Fig. 2. *Command following for the linearized two-link system:* The adaptive control (27)-(29) uses knowledge of the nonminimum-phase zero to track a sinusoid with unknown frequency and amplitude. The adaptive control is turned on after 7.5 seconds and drives the performance to zero.

Next, we implement the adaptive controller in feedback with nonlinear plant, using the estimate of the nonminimum-phase zero obtained from the linearized two-link system. Figure 3 shows that the adaptive controller drives the performance variable z toward zero, and the performance is comparable to the linear case shown in Figure 2.

We simulated the nonlinear two-link system with physical parameters given in Section IV and the adaptive controller in feedback for various command amplitudes, and we found that the adaptive controller is able to drive z toward zero for all command amplitudes less than 0.4 rad (or 23 degrees).

Next, we consider the disturbance rejection problem, where the control objective is to drive θ_2 to zero, while a 1.6 Hz sinusoidal disturbance is applied at both p_1 and p_2. The magnitudes of the disturbances at p_1 and p_2 are 0.2 rad and 0.4 rad, respectively. We assume that the relative degree d, the first nonzero Markov parameter, and the location of the nonminimum-phase zero are known, but no other information about the system is assumed to be known. Figure 4 shows that the adaptive controller is able to reject the disturbance from θ_2, and thus drives z to zero.

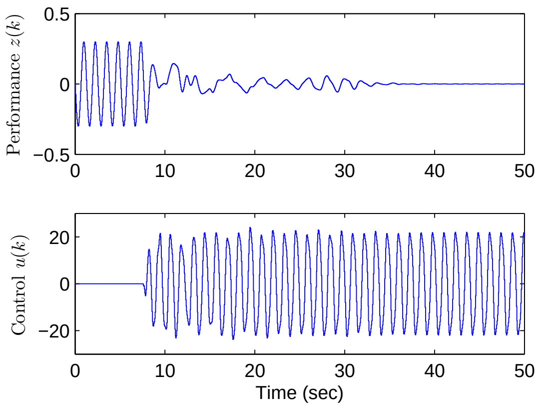

Fig. 3. *Command following for the nonlinear two-link system:* The adaptive control (27)-(29) uses knowledge of the linearized nonminimum-phase zero to track a sinusoid with unknown frequency and amplitude. The adaptive control is turned on after 7.5 seconds and drives the performance to zero. The performance with the nonlinear system is comparable to the linear case shown in Figure 2.

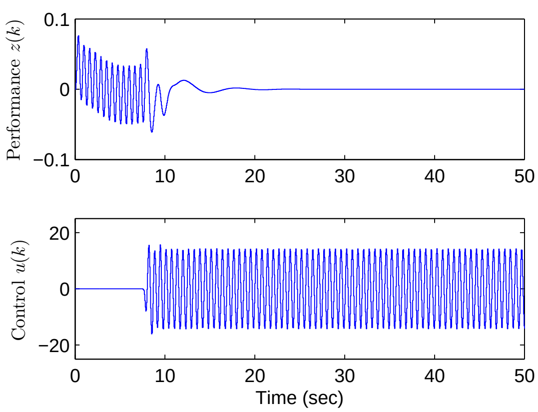

Fig. 4. *Disturbance rejection for the linearized two-link system:* The adaptive control (27)-(29) uses knowledge of the nonminimum-phase zero to reject an unknown sinusoidal disturbance acting on both joints of the two-link mechanism. The adaptive control is turned on after 7.5 seconds and drives the performance to zero.

Next, we implement the adaptive controller in feedback with nonlinear plant, using the estimate of the nonminimum-phase zero obtained from the linearized two-link system. Figure 5 shows that the adaptive controller drives z toward zero, and the performance is comparable to the linear case shown in Figure 4.

VII. Conclusion

In this paper, we investigated a nonlinear planar multi-link mechanism that is interconnected by torsional springs and dashpots. More specifically, we considered a nonlinear multilink mechanism where a control torque is applied to the hub of the multilink mechanism, and the objective is to control the angular position of the tip, which is separated from the hub by N links. We derived the nonlinear equations of motion, linearized these equations of motion, and demonstrated that the linear transfer function from the hub to the tip of the multilink mechanism has $N-1$ nonminimum-phase zeros. Finally, we implemented a retrospective cost adaptive controller [6] to control the multilink mechanism. We demonstrated both command following and disturbance rejection where commands and disturbances had unknown spectra.

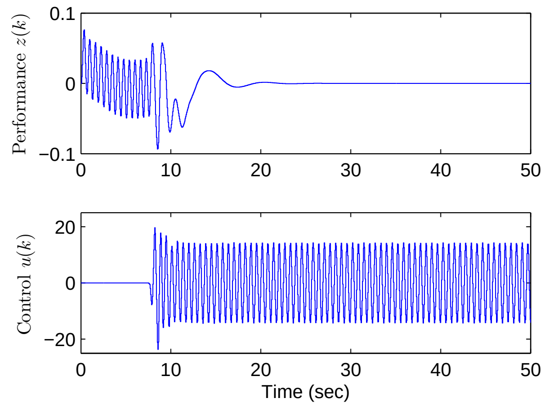

Fig. 5. *Disturbance rejection for the nonlinear two-link system:* The adaptive control (27)-(29) uses knowledge of the nonminimum-phase zero to reject an unknown sinusoidal disturbance acting on both joints of the two-link mechanism. The adaptive control is turned on after 7.5 seconds and drives the performance to zero. The performance with the nonlinear system is comparable to the linear case shown in Figure 4.

References

[1] H. Kwakernaak and R. Sivan, *Linear Optimal Control Systems*. Wiley, 1972.
[2] S. Skogestad and I. Postlethwaite, *Multivariable Feedback Control*, 2nd ed. New York: Wiley, 2005.
[3] J. B. Hoagg and D. S. Bernstein, “Nonminimum-phase zeros: Much to do about nothing,” *IEEE Contr. Sys. Mag.*, vol. 27, pp. 45–57, June 2007.
[4] P. Ioannou and B. Fidan, *Adaptive Control Tutorial*. Philadelphia: SIAM, 2006.
[5] M. A. Santillo and D. S. Bernstein, “Adaptive control based on retrospective cost optimization,” *AIAA J. Guid. Contr. Dyn.*, vol. 33, pp. 289–304, 2010.
[6] J. B. Hoagg and D. S. Bernstein, “Cumulative retrospective cost adaptive control with RLS-based optimization,” in *Proc. Amer. Contr. Conf.*, Baltimore, MD, June 2010, pp. 4016–4021.
[7] J. Hong and D. S. Bernstein, “Bode integral constraints, colocation, and spillover in active noise and vibration control,” *IEEE Trans. Contr. Sys. Tech.*, vol. 6, pp. 111–120, 1998.
[8] J. B. Hoagg, J. Chandrasekar, and D. S. Bernstein, “On the zeros, initial undershoot, and relative degree of lumped-mass structures,” *ASME J. Dynamical Systems, Measurement, and Contr.*, vol. 129, pp. 493–502, 2007.
[9] D. K. Miu, *Mechatronics*. New York: Springer-Verlag, 1993.
[10] E. H. Maslen, “Positive real zeros in flexible beams,” *Shock and Vibration*, vol. 2, no. 6, pp. 429–435, 1995.
[11] D. Abramovitch and G. Franklin, “A brief history of disk drive control,” *IEEE Contr. Sys. Mag.*, vol. 22, no. 3, pp. 28–42, 2002.
[12] B. P. Rigney, L. Y. Pao, and D. A. Lawrence, “Nonminimum phase dynamic inversion for settle time applications,” *IEEE Trans. Contr. Sys. Tech.*, vol. 17, pp. 989–1005, 2009.
[13] M. S. Fledderjohn, M. S. Holzel, A. V. Morozov, J. B. Hoagg, and D. S. Bernstein, “On the accuracy of least squares algorithms for estimating zeros,” in *Proc. Amer. Contr. Conf.*, Baltimore, MD, June 2010, pp. 3729–3734.
[14] G. C. Goodwin and K. S. Sin, *Adaptive Filtering, Prediction, and Control*. Prentice Hall, 1984.
[15] K. J. Åström and B. Wittenmark, *Adaptive Control*, 2nd ed. Addison-Wesley, 1995.
[16] G. Tao, *Adaptive Control Design and Analysis*. Wiley, 2003.